Effects of BOF Top-blowing and Bottom-stirring Conditions on Suppressing Excessive Oxidation

Ken-ichiro Naito*, Shin-ya Kitamura and Yuji Ogawa****

*** Ken-ichiro Naito was formerly a senior researcher at Steel Research Laboratories, Nippon Steel Corporation, and now is a guest researcher at the Division of Metallurgy.**
Royal Institute of Technology (KTH)
Department of Material Science and Engineering
Division of Metallurgy
SE-100 44 Stockholm, Sweden
Fax: +46-8 790 0939
Tel: +46-8 790 9568

**** Shin-ya Kitamura is a chief researcher and Yuji Ogawa is a senior researcher at Steel Research Laboratories.**
Nippon Steel Corporation
Steel Research Laboratories
20-1, Shintomi, Futtsu, Chiba, 293-8511, Japan

Key Words: BOF steelmaking, top-blowing, bottom-stirring, decarburization, oxidation, mass transfer, model.

Abstract

To suppress excessive oxidation in BOF steelmaking, the effects of top-blowing and bottom-stirring conditions were investigated in a 6t converter. Under the condition with low oxygen feeding rate and high stirring energy, the apparent partial pressure of CO gas calculated from the equilibrium of carbon and oxygen in molten steel (=P_{CO}') was suppressed below 1atm. The experimental results were analyzed from the viewpoint of the relation between top-blowing / bottom-stirring conditions and the mass transfer at slag-metal interface. The mass transfer at hot spot is suggested to be significantly affected by the reaching oxygen rate to steel bath and the bottom-stirring, while the mass transfer at slag-metal interface outside of the hot spot is large enough to attain equilibrium in combined-blowing BOF processes. This means that the oxygen that is not consumed for decarburization is distributed between the bulk bath and slag, i.e. deoxidation from the bulk bath to slag takes place, which enables to obtain lower P_{CO}' than 1atm under atmospheric condition. The decarburization model developed based on the analysis reproduces the suppression of excessive oxidation under decreased top-blown oxygen feeding rate and is in good agreement with both 6t converter experiments and 350t commercial BOF operation.

1. INTRODUCTION

It has been about two decades since the BOF combined-blowing process, which consists of top-blowing and bottom-stirring, was introduced because of its high refining ability especially from the viewpoint of suppressing excessive oxidation. In combined-blowing BOF steelmaking, several refining indexes such as ISCO[1)] and BOC[2)] have been proposed so far and the oxygen feeding rate is usually controlled based on these indexes during the last stage of blowing. For example, BOC is described by,

$$BOC = \frac{Q_{O2}}{(W/t)\cdot[C]} \quad \cdots\cdots\cdots(1)$$

where Q_{O2} is oxygen feeding rate (Nm^3/min), W is weight of molten steel (t), is mixing time (sec) and [C] is the concentration of carbon in the molten steel (wt%).

Equation (1), in which the denominator and the numerator respectively represent the rate of carbon and oxygen supply, means the ratio of two reactants supplied to the reaction site. It has been reported that excessive oxidation, e.g. the concentration of dissolved oxygen in molten steel and the concentration of total iron in slag, tends to be more suppressed at smaller value of BOC[2)].

Bergman[3)] conducted experiments for directly producing low-carbon-steel in a 6t converter equipped with a low flow rate lance and a bottom-stirring system, and reported that the apparent partial pressure of CO gas calculated from the equilibrium of carbon and oxygen in molten steel was below 0.4atm in most of the experiments. This means that suppressing excessive oxidation to the considerably lower level is possible under appropriate operating conditions.

Optimization of operating conditions, however, is not completely established since the effect of combined-blowing on stirring conditions is still quantitatively unclear. Okohira et al.[4)] reported using a water model that the contribution of top-blown energy to stirring was only 10% of the total kinetic energy of the top-blown jet. However, the energy supplied from CO gas generation was not taken into consideration, which means cold model experiments are not sufficient to properly simulate and evaluate stirring conditions. Furthermore, the mixing property was evaluated only from the viewpoint of macro mixing that is represented by mixing time, while micro mixing at the slag-metal interface in a combined-blowing BOF has been studied less.

In this study, the effects of top-blowing and bottom-stirring conditions on suppressing excessive oxidation were investigated in a 6t converter and the experimental results were analyzed from the viewpoint of the relation between top-blowing / bottom-stirring conditions and the mass transfer at the slag-metal interface i.e. the stirring condition at the slag-metal interface. Based on this analysis, the effects of the top-blowing and bottom-stirring were estimated quantitatively and a model was developed by modifying the model proposed by Kishimoto et al.[5)].

2. EXPERIMENTAL PROCEDURE

About 6t pig iron was melted in an induction furnace, charged into the pilot-scale converter and decarburization experiments were conducted. Lime was added just after the beginning of blowing so that the value of (wt%CaO)/(wt%SiO_2) became about 3.5 according to the concentration of silicon in the pig iron.

At the last stage of blowing when the concentration of carbon reached the specified value (0.4wt%), the top-blown oxygen feeding rate, the height of lance from the steel bath and the bottom-stirring gas flow rate were set to the appointed values in each experiment. In several experiments, nitrogen gas was added to the top-blown oxygen aiming at enhancing the stirring and promoting the mass transfer at hot spot where oxygen jet collide with the steel bath.

Samples of molten steel and slag were taken by a sublance and the concentrations of carbon (=[C](wt%)), dissolved oxygen (=[O](wt%)) in molten steel and total iron in slag (=(T.Fe)(wt%)) were determined to investigate the behavior of oxidation during the last stage of blowing. The conditions are shown in Table 1.

3. RESULTS

The changes in [C] and [O] classified by top-blown oxygen feeding rate are shown in Figure 1. The bottom-stirring energy is between 3.0 and 3.4kW/t and the top-blown oxygen feeding rates are 1200, 400 and 250Nm^3/h. (Since ordinary top-blown oxygen feeding rate in commercial BOF is approximately 200Nm^3/h/t, the condition of 1200Nm^3/h corresponds to ordinary operation.) In the figure, the lines show the equilibrium of [C] and [O] at each partial pressure of CO gas calculated from,

$$\underline{C} + \underline{O} = CO_{(g)} \qquad \cdots\cdots\cdots (2)$$

$$P_{CO} = 10^{(1160/T+2.003)} a_C a_O \approx 10^{(1160/T+2.003)} [C][O] \qquad \cdots\cdots\cdots (3)^{6)}$$

where P_{CO} is partial pressure of CO gas (atm), a_C and a_O are the activities of carbon and oxygen in molten steel respectively and T is temperature (K). The correction of activity is negligible since the activity coefficients of both carbon and oxygen are almost unity in this system.

The figure shows that [O] increases with the decrease of [C] under all conditions. While the changes of [C] and [O] are similar under every condition at higher [C] than 0.2wt%, the increase of [O] is more suppressed under the conditions with lower top-blown oxygen feeding rate at lower [C] than 0.05wt%. It should also be noted that the apparent partial pressure of CO gas calculated from the equilibrium of [C] and [O] (=P_{CO}') is suppressed below 1atm.

The effects of the top-blown oxygen feeding rate and mixing time on the minimum value of P_{CO}' during blowing period (=$P_{CO', min}$) are shown in Figure 2 and 3, respectively. Mixing time is calculated from the bottom-stirring energy as follows,

$$t_s = 100 \left\{ \frac{\left(D^2/H\right)^2}{e_B} \right\}^{0.337} \qquad \cdots\cdots\cdots (4)^{7)}$$

$$e_B = \frac{103QT}{W_m} \left\{ \ln\left(1 + \frac{9.8rH}{P}\right) + 0.06\left(1 - \frac{T_n}{T}\right) \right\} \qquad \cdots\cdots\cdots (5)^{8)}$$

where $_s$ is mixing time (sec) that is defined as 95% bulk mixing, D is diameter of refining vessel (m), H is bath depth (m), $_B$ is bottom-stirring energy (W/t), Q is efficient flow rate of bottom-stirring gas[4] (Nm^3/h), W_m is weight of molten steel (kg), is density of molten steel (kg/m^3), P is atmospheric pressure (Pa) and T_n and T are temperature of injected gas and molten steel, respectively (K).

$P_{CO,\,min}^{'}$ becomes lower with the decrease of the top-blown oxygen feeding rate and also with the decrease of mixing time, which means the oxidation is affected not only by the equilibrium between [C] and [O] but also by the supplying rate of carbon and oxygen to the reaction site. The conditions under which nitrogen was added into top-blown oxygen are also plotted in Figure 2. The figure shows that the addition of nitrogen neither promotes decarburization nor suppresses oxidation. These results indicate that it is important to decrease the top-blown oxygen feeding rate and to enhance bottom-stirring in order to suppress excessive oxidation. However, the addition of inert gas into the top-blown oxygen does not seem to effectively affect the enhancement of mass transfer.

4. DISCUSSION

4.1. Decarburization mechanism in BOF

Kishimoto et al.[5] proposed a mathematical decarburization model at low carbon concentration region in the BOF as illustrated in Figure 4. The following assumptions are adopted.

1) Molten steel in the BOF is comprised of two zones, one of which is the reaction zone (=hot spot where oxygen jet collide with the steel bath) and the other is the bulk bath zone. The volume of the reaction zone is negligibly small compared to the bulk bath zone. The molten steel carried into the reaction zone by circulation flow reacts with oxygen jet, returns to the bulk bath zone and completely mixes with the bulk bath.

2) The activity of FeO in the reaction zone (=a_{FeO}) is unity since oxygen is sufficiently supplied in this zone. The equilibrium is attained at the interface between molten steel and FeO in the reaction zone.

3) The rest of the supplied oxygen that is not consumed for decarburization accumulates in the bulk bath zone as dissolved oxygen or in slag as FeO. The mass transfer of oxygen takes place between the bulk bath zone and slag according to the difference of oxygen potential.

In the figure, q is circulation flow rate in the bulk bath zone (kg/min), k is mass transfer coefficient (m/min), A is interfacial area (m^2), small notation b, r, s and * attached to bracket [], T or a_{FeO} mean the bulk bath zone, reaction zone, slag and equilibrium state, respectively, and small notation 1 and 2 attached to k or A mean the slag-metal interface in the reaction zone and slag-metal interface outside of the reaction zone, respectively. Although Kishimoto et al. describe the products of mass transfer coefficients, interfacial areas and density (=k_1A_1 and k_2A_2) as “mixing factors” (=I and J) in their original model, the description is substituted as above in order to make its physical meaning clearer.

In this model, the kinetic parameters are q, k_1A_1 and k_2A_2 , and the parameter q is calculated from,

$$q = 60 \cdot \ln\left(\frac{1}{1-0.95}\right)\frac{W_m}{t} \approx \frac{180W_m}{t} \qquad \cdots\cdots\cdots(6)^{7)}$$

Therefore, the unknown parameters in this model are k_1A_1 and k_2A_2 , and they are presumed to be affected by the mixing conditions at the slag-metal interface caused by the combined top-blowing and bottom-stirring conditions. However, quantitative effects of top-blowing and bottom-stirring on these parameters were not sufficiently investigated by Kishimoto et al. In the following sections, these parameters k_1A_1 and k_2A_2 are discussed based on the experimental results.

4.2. Effect of top-blowing on the mass transfer at slag-metal interface in the reaction zone

The unknown parameters k_1A_1 is discussed in this section.

The following equations can be derived from the assumptions described in the previous section,

$$W_m \frac{d[C]_b}{dt} = \frac{qk_1A_1r}{q+k_1A_1r}\left([C]^* - [C]_b\right) = KW_m\left([C]^* - [C]_b\right) \quad \cdots\cdots\cdots(7)$$

$$\frac{1}{KW_m} = \frac{1}{q} + \frac{1}{k_1A_1r} \quad \cdots\cdots\cdots(8)$$

where t is time (min) and K is overall volumetric coefficient of mass transfer (1/min).

As shown in Figure 5, it is well known that the decarburization rate is determined by the mass transfer rate of carbon at low carbon concentration region, while it is determined by the oxygen feeding rate at high carbon concentration region. Therefore, there is a point where the rate determining step changes from the oxygen feeding rate to mass transfer rate of carbon. The concentration of carbon at the transition point is called $[C]_B$(wt%) The oxygen feeding rate is equal to the mass transfer rate of carbon at $[C]_B$ and this is described by,

$$100 \cdot h \frac{F_{O2}}{60}\frac{12}{11.2} = KW_m\left([C]_B - [C]^*\right) \quad \cdots\cdots\cdots(9)$$

where is reaching efficiency of top-blown oxygen to the steel bath that excludes the oxygen consumed for post combustion (-) and F_{O2} is the top-blown oxygen feeding rate (Nm^3/h),

The value of $[C]^*$ calculated from the assumption that a_{FeO} is unity at high temperature of hot spot (2000°~2600°C) [9] is found to be negligibly small and can be determined from the post combustion ratio during experiments. Therefore, by determining $[C]_B$ by extrapolating the decarburization rate at the low carbon concentration region, the value of K can be calculated from Equation (9). Then, the value of k_1A_1 for each condition can be calculated by substituting K in Equation (8),

The relations between k_1A_1 and top-blowing conditions, i.e. the jet velocity at the centerline[10] and the products of reaching efficiency and top-blown oxygen feeding rate (= F_{O2}), are plotted in Figures 6 and 7, respectively. As shown in the figures, there is a good correlation between k_1A_1 and F_{O2}, while there is no correlation between k_1A_1 and the jet velocity even under the conditions with nitrogen gas addition, which means that the effect of F_{O2}, i.e. the effect of reaching oxygen to the steel bath, on enhancing the mass transfer in the reaction zone is much higher than that of the kinetic energy of the jet. Presumably, the energy generated by CO gas as the product of decarburizaton reaction mainly contributes to the stirring condition in the reaction zone and the kinetic energy of the jet is comparatively less influential. By assuming that k_1A_1 is proportional to the powers of F_{O2}, the exponent is found to be within the range from 0.5 to 0.7 as shown in Figure 7. This is described as follows,

$$k_1A_1r \propto (hF_{O2})^{0.5\sim0.7} \quad \cdots\cdots\cdots(10)$$

4.3. Effect of bottom-stirring on the mass transfer at slag-metal interface in the reaction zone

In the previous section, the contribution of top-blowing to the parameters k_1A_1 is discussed. On the contrary, the contribution of bottom-stirring to the parameters k_1A_1 is not clear in Figure 7, since it is impossible to change the circulation flow rates in a wide range in a particular vessel scale and the effect of bottom-stirring is vague in the scattered data. However, it is well known that bottom-stirring also promotes the mass transfer at the slag-metal interface[11] and it undoubtedly affects the stirring condition at slag-metal interface in the reaction zone, i.e. the parameter k_1A_1 , although the quantitative determination from the data of this work is impossible.

Therefore, assuming that k_1A_1 is proportional to the powers of F_{O2} and q, we estimated the effect of bottom-stirring on the parameter k_1A_1 by regression analysis based on the data of 6t converter experiments and 350t commercial BOF operation and obtained following equation,

$$k_1A_1 r = 0.0109(hF_{O2})^{0.652} q^{0.713} \quad \cdots\cdots\cdots (11)$$

This equation suggests that the effect of bottom-stirring on the parameter k_1A_1 is also significant. In addition, the effect of top-blowing on the parameter k_1A_1 , i.e. the exponent of F_{O2}, is consistent with Equation (10).

On the other hand, it should be noted that bottom-stirring plays an important role in carrying the bulk bath into the reaction zone and enhancing the overall mass transfer of molten steel as formulated in Equation (8).

4.4. Mass transfer at slag-metal interface outside of the reaction zone

The unknown parameter k_2A_2 is discussed in this section.

Since the parameter k_2A_2 represents the mass transfer of oxygen at slag-metal interface outside of the reaction zone, i.e. the mass transfer at the interface between the slag and the bulk bath, the deviation from the oxygen equilibrium between two phases should be investigated.

The relation between [O] and (T.Fe), including the data of 6t converter experiments and 350t commercial BOF operation, is shown in Figure 8. The lines in the figure show the calculated equilibrium of [O] and (T.Fe) ((T.Fe) is converted into (FeO), and the activity coefficient of FeO (= $_{FeO}$) is assumed to be 1.1~1.5 from the work by Turkdogan[12] under the condition of (wt%CaO)/(wt%SiO_2) 3.5). This figure indicates that the oxygen potential of the bulk bath and slag is almost equal, which means the mass transfer at slag-metal interface outside of the reaction zone is large enough to attain equilibrium in combined-blowing BOF processes. Therefore, by assuming that the rest of the supplied oxygen that is not consumed for decarburization is distributed between bulk bath and slag so as to attain oxygen distribution equilibrium instantaneously, the following equations can be adopted and k_2A_2 does not need to be determined.

$$W_m \frac{d[O]_b}{dt} + \frac{d\{W_s(FeO)\}}{dt}\frac{16}{71.9} = 100 \cdot h \frac{F_{O2}}{60}\frac{16}{11.2} - W_m \frac{d[C]_b}{dt}\frac{16}{12} \quad \cdots\cdots\cdots (12)$$

$$[O]_b = 10^{(-6150/T_b + 2.604)} g_{FeO} \frac{\dfrac{(FeO)}{71.9}}{\dfrac{(FeO)}{71.9} + \dfrac{(CaO)}{56.1} + \dfrac{(SiO_2)}{60.1}} \quad \cdots\cdots\cdots (13)^{6)}$$

where W_s is weight of slag (kg) and the other components than FeO, CaO and SiO_2 in slag are disregarded.

4.5. Effects of top-blowing and bottom-stirring on suppressing excessive oxidation

As shown in Figures 1~3, the apparent partial pressure of CO gas calculated from the equilibrium of [C] and [O] ($=P_{CO}'$) was more suppressed below 1atm under the condition with lower top-blown oxygen feeding rate and higher bottom-stirring energy. This means that [C] and [O] are not simply determined by the equilibrium at the bulk bath. The mechanism of decarburization and oxidation in BOF can be explained as follows:

1) The molten steel returned from the reaction zone to the bulk bath includes a low content of carbon and a high content of oxygen.

2) While the carbon is directly returned to the bulk bath, the oxygen is not directly returned to the bulk bath but distributed between the bulk bath and slag, i.e. deoxidation from the bulk bath to slag takes place. [O] is determined by the oxygen distribution equilibrium between bulk bath and slag, not by the equilibrium of [C] and [O] in the bulk bath.

3) Under the condition with low top-blown oxygen feeding rate and high bottom-stirring energy, while the oxygen consumed for decarburization increases, the rest of the oxygen that is consumed for FeO generation or dissolved oxygen decreases, which enables to obtain lower P_{CO}' than 1atm under atmospheric condition.

Although the contribution of bottom-blown nitrogen gas to the dilution of actual P_{CO} in the system might be pointed out, it was reported that the effect of inert gas on lowering P_{CO}' was not significant in the experiments in which the CO_2 and Ar as bottom-stirring gas were compared[4), 5)].

4.6. Simulation by the modified decarburization model

The simulation results by the modified decarburization model are shown in Figures 9, 10 and 11. This model reproduces the suppression of excessive oxidation under decreased top-blown oxygen feeding rate and is in good agreement with both 6t converter experiments and 350t commercial BOF operation.

On the other hand, as described in Equations (10) and (11), since top-blown oxygen plays an important role in promoting the mass transfer at the slag-metal interface in the reaction zone, the decrease of the top-blown oxygen feeding rate will cause the lowering of the decarburization rate as shown Figure 11 and will result in the prolongation of blowing time. In order to prevent this, the increase of bottom-blowing energy is supposed to be effective, although its effect on the mass transfer at the slag-metal interface under combined-blowing condition needs further study.

5. CONCLUSIONS

1) In order to suppress excessive oxidation, it is important to decrease the top-blown oxygen feeding rate and to enhance bottom-stirring energy. Under the condition with low top-blown oxygen feeding rate and high bottom-stirring energy, the apparent partial pressure of CO gas calculated from the equilibrium of carbon and oxygen in molten steel ($=P_{CO}$') was suppressed below 1atm.

2) It is presumed that the energy generated by CO gas as the product of decarburizaton reaction mainly contributes to the stirring condition in the reaction zone and that the kinetic energy of the jet is comparatively less influential.

3) By assuming that the mass transfer parameter at the slag-metal interface in the reaction zone (=k_1A_1) is proportional to the powers of reaching oxygen rate to steel bath (= F_{O2}), the exponent is found to be within the range from 0.5 to 0.7.

4) The effect of bottom-stirring on the parameter k_1A_1 was estimated by regression analysis based on the data of 6t converter experiments and 350t commercial BOF operation, and it is suggested to be also significant.

5) The oxygen potential of the bulk bath and slag is almost equal, which means the mass transfer at slag-metal interface outside of the reaction zone is large enough to attain equilibrium in combined-blowing BOF processes.

6) The oxygen that is not consumed for decarburization is distributed between the bulk bath and slag, i.e. deoxidation from the bulk bath to slag takes place. Under the condition with low top-blown oxygen feeding rate and high bottom-stirring energy, the oxygen that is consumed for FeO generation or dissolved oxygen decreases, which enables to obtain lower P_{CO}' than 1atm under atmospheric condition.

7) The developed model reproduces the suppression of excessive oxidation under decreased top-blown oxygen feeding rate and is in good agreement with both 6t converter experiments and 350t commercial BOF operation.

8) Since top-blown oxygen plays an important role in promoting the mass transfer at the slag-metal interface in the reaction zone, the decrease of the top-blown oxygen feeding rate will result in the prolongation of blowing time. In order to prevent this, the increase of bottom-blowing energy is supposed to be effective, although its effect on the mass transfer at the slag-metal interface under combined-blowing condition needs further study.

REFERENCES

1) Y. Kato, K. Nakanishi and T. Nozaki: *Japan-Sweden Joint Symposium on Ferrous Metallurgy*, (1978).
2) T. Kai, K. Okohira, M. Hirai, S. Murakami and N. Sato: *Tetsu-to-Hagané*, 68 (1982), 1946.
3) D. Bergman: *SCANINJECT VI*, (1992), 417
4) K. Okohira, M. Hirai, S. Murakami and T. Kai: *Seitetsu-Kenkyu*, 314 (1984), 91.
5) Y. Kishimoto, Y. Kato, T. Sakuraya and T. Fujii: *Tetsu-to-Hagané*, 75 (1989), 1300.
6) 19th Steelmaking Committee: Recommended Equilibrium Values for Steelmaking Reactions, Japan Society for Promotion of Science, Japan (1984).
7) M. Sano and K. Mori: *Tetsu-to-Hagané*, 68 (1982), 2451.
8) K. Mori and M. Sano: *Tetsu-to-Hagané*, 67 (1981), 672.
9) K. Kawakami: *Tetsu-to-Hagané*, 74 (1988), 831.
10) K. Naito, Y. Ogawa, T. Inomoto, S. Kitamura and M. Yano: *ISIJ Int.*, 40 (2000), 31.
11) K. Nakanishi, Y. Kato, T. Nozaki and T. Emi: *Tetsu-to-Hagané*, 66 (1980), 1307.
12) E. T. Turkdogan: *Turkdogan Symposium Proceedings*, (1994), 253.

FIGURES

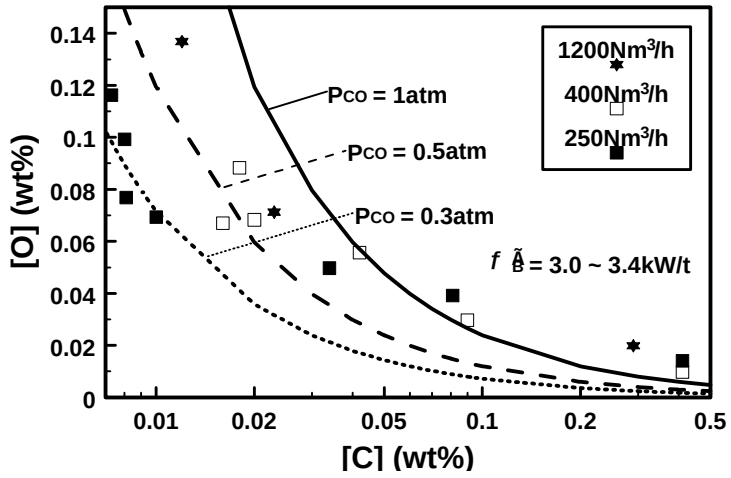

Figure 1. Changes in [C] and [O] classified by top-blown oxygen feeding rate.

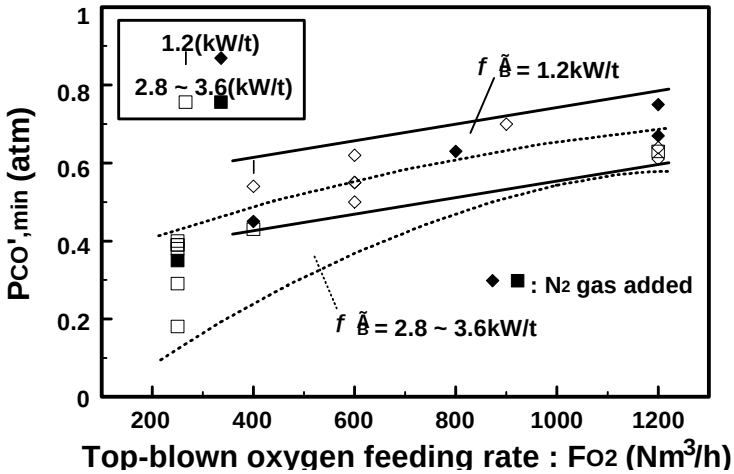

Figure 2. Effect of top-blown oxygen feeding rate on $P_{CO',min}$.

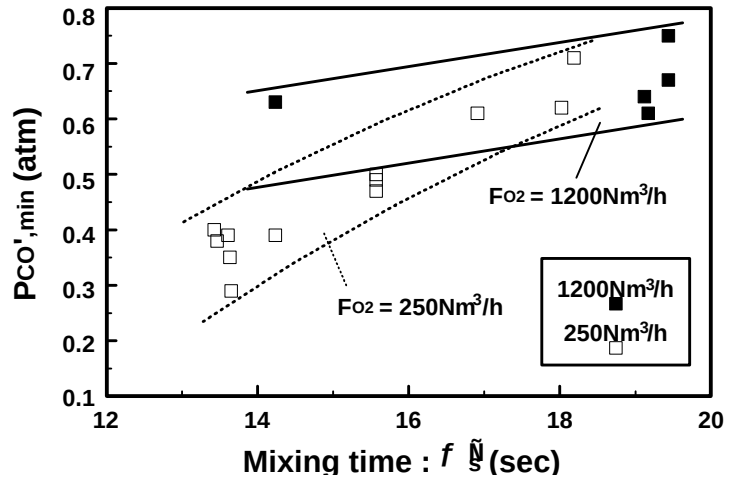

Figure 3. Effect of mixing time on $P_{CO',min}$.

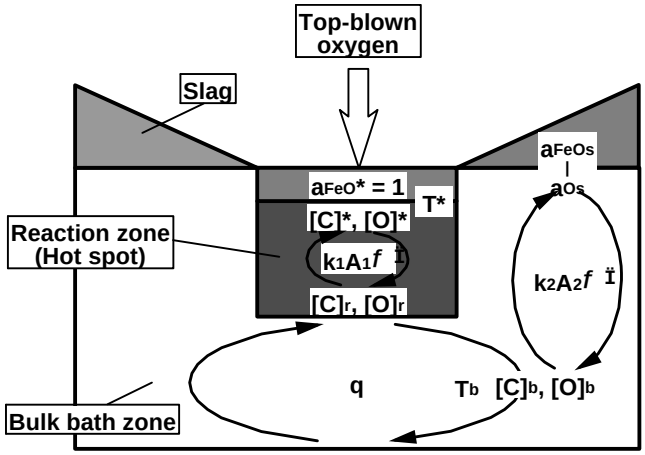

Figure 4. Schematic diagram of decarburization model in BOF[5].

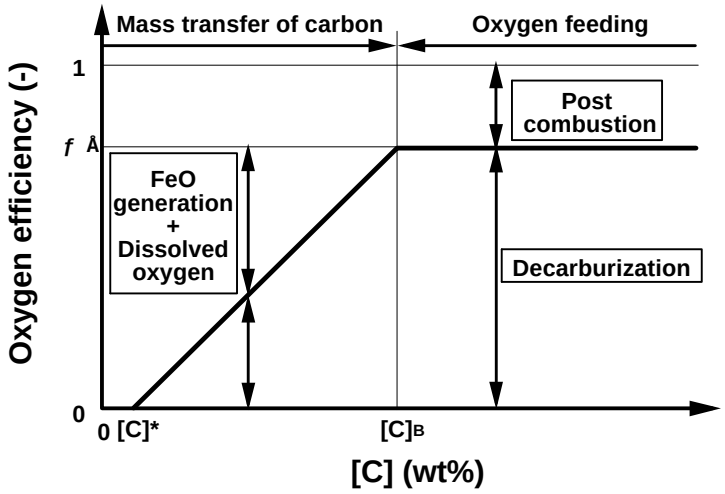

Figure 5. Rate determining step of decarburization reaction.

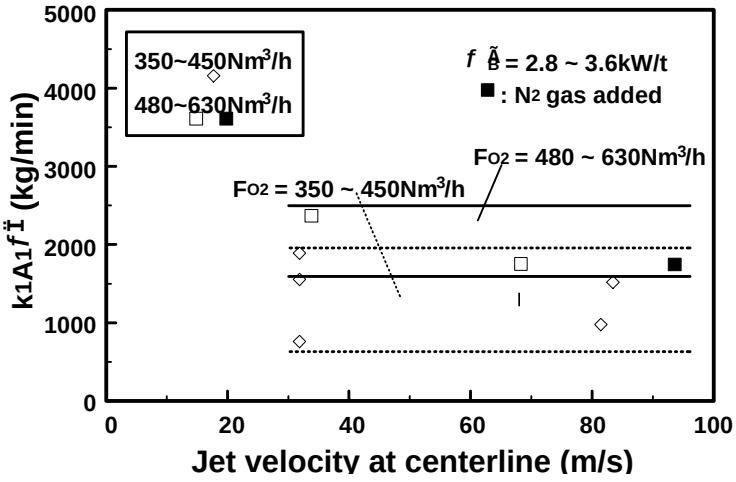

Figure 6. Relation between jet velocity at centerline and k_1A_1 .

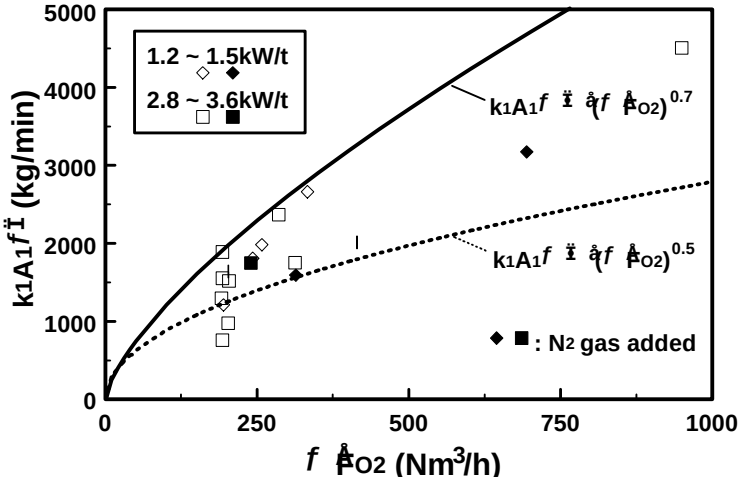

Figure 7. Relation between F_{O2} and k_1A_1 .

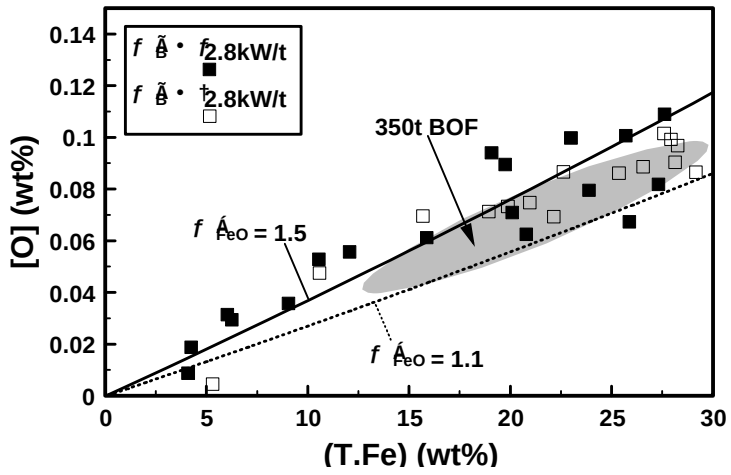

Figure 8. Relation between [O] and (T.Fe).

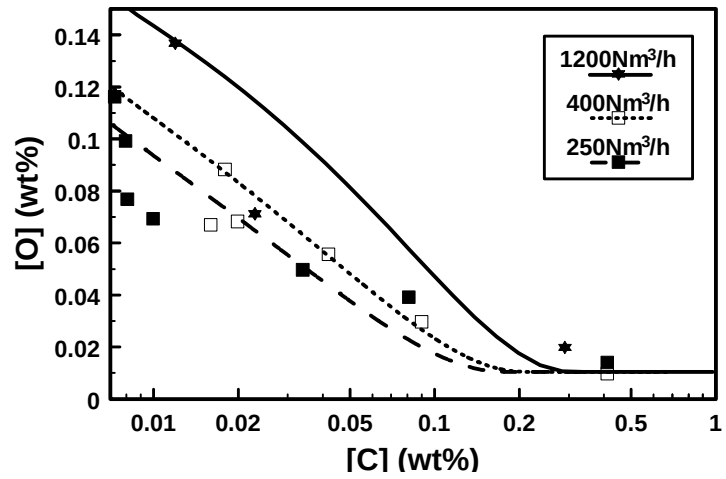

Figure 9. Comparison of calculated and measured values of [C] and [O] (6t).

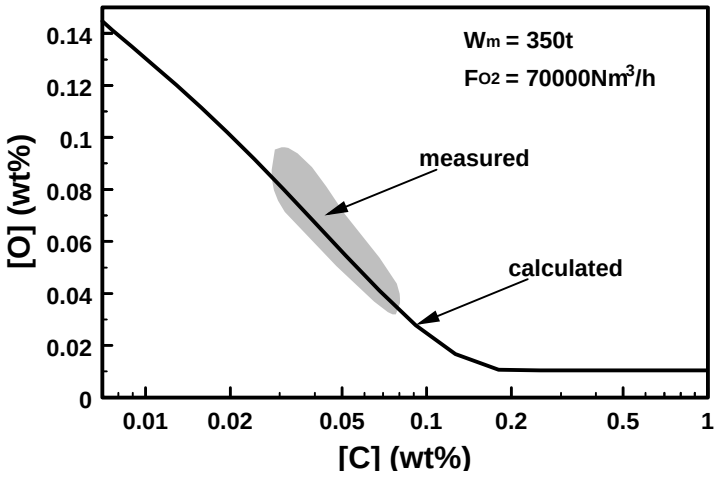

Figure 10. Comparison of calculated and measured values of [C] and [O] (350t).

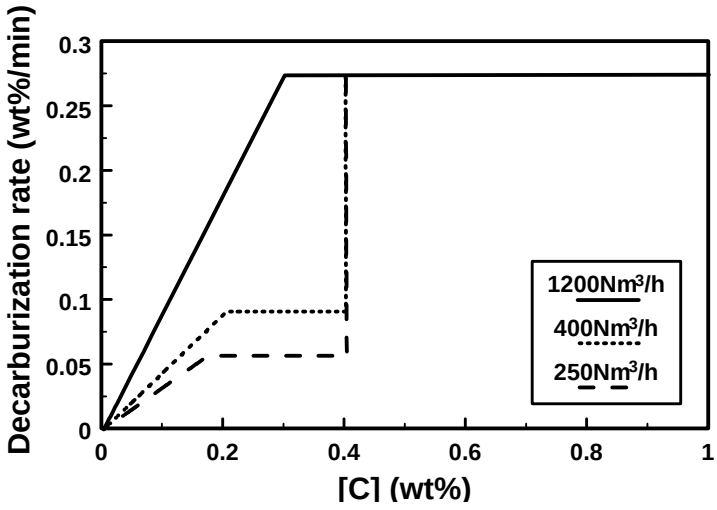

Figure 11. Calculated decarburization rate.

TABLES

Table 1. Experimental conditions.

Weight of initial pig iron	6t
Weight of initial slag	30kg/t
Top-blown oxygen feeding rate	250~1200Nm^3/h
Top-blown nitrogen feeding rate	0~500Nm^3/h
Height of lance	650~1000mm
Bottom-stirring gas and flow rate	N_2: 100~250Nm^3/h
Bottom-stirring energy	1.2~3.6kW/t